JSR Publications

Available Online

J. Sci. Res. **13** (1), 21-29 (2021)

JOURNAL OF SCIENTIFIC RESEARCH

www.banglajol.info/index.php/JSR

Phonon Dynamics and Acoustic and Thermodynamic Properties of $Pt_{57.5}Cu_{14.7}Ni_{5.3}P_{22.5}$ Bulk Metallic Glass

R. R. Koireng[1,2*], P. C. Agarwal[3], A. Gokhroo[1]

[1]Samrat Prithviraj Chauhan Government College, Ajmer-305001, Rajasthan, India

[2]National Institute of Education (NCERT), New Delhi-110016, India

[3]Regional Institute of Education (NCERT), Bhubaneswar-751022, Odisha, India

Received 2 June 2020, accepted in final revised form 29 September 2020

Abstract

The phonon dispersion curves for $Pt_{57.5}Cu_{14.7}Ni_{5.3}P_{22.5}$ bulk metallic glass (BMG) are computed employing various dielectric screenings using the simple model given by Bhatia and Singh. The force constants β and δ for computing the dispersion curves are calculated from the elastic constants i.e. bulk modulus (B) and shear modulus (G) along with the calculated value of force constant κ_e of the material of the glass for the first time. The results of the phonon dispersion curves show appropriate behavior in the long wavelength region in detail for both the longitudinal and transverse modes and give insight regarding the acoustic and thermal properties of the BMG. The transverse sound velocity and the longitudinal velocities with various dielectric screening are calculated from the dispersion curves in the long wavelength region. The corresponding thermodynamic property (Debye temperature) is calculated for different dielectric screenings. The theoretical results predicted are in a good agreement with the reported data in the literature for the $Pt_{57.5}Cu_{14.7}Ni_{5.3}P_{22.5}$ BMG and may be used for correlating other properties.

Keywords: Bulk metallic glass; Phonon dispersion; Dielectric screening; Elastic constant.

doi: http://dx.doi.org/10.3329/jsr.v13i1.47327 J. Sci. Res. **13** (1), 21-29 (2021)

1. Introduction

Bulk metallic glasses have emerged with attractive mechanical and thermal properties having a wide range of technological applications [1,2]. The understanding of phonon dynamics and micro-structural configuration of metallic glasses is essential for understanding their acoustic, elastic and thermal properties [2–7]. Experimentally, neutron scattering has been used to study the phonon frequencies of metallic glasses [8,9]. The theoretically computed phonon dispersion curves both for longitudinal and transverse modes have also been reported by computer simulation and recursion techniques [8-13]

* *Corresponding author*: karenkrr@gmail.com

for a variety of metallic glasses. Three main theoretical approaches, namely Hubbard and Beeby [14], Takeno and Goda [15] and that of Bhatia and Singh [4] are widely used for computing phonon frequencies of metallic glasses. Pratap *et al.* [16] has computed phonon frequencies of $Cu_{57}Z_{43}$ metallic glass using both Hubbard and Beeby and that of Takeno and Goda approaches. Vora and Gandhi [13] have reported phonon dispersion curves of $Pd_{39}Ni_{10}Cu_{30}P_{21}$ using Takeno and Goda approach. The simple model approach by Bhatia and Singh [4] has been applied for computing phonon dispersion of various metallic glasses-$Cu_{57}Zr_{43}$ by Agarwal *et al.* [7], for Zr–Ni alloys by Lad and Pratap [17] and by Agarwal for Zr-Ti-Cu-Ni-B [10] and $Cu_{60}Zr_{20}Hf_{10}Ti_{10}$ [11] bulk metallic glasses (BMGs).

$Pt_{57.5}Cu_{14.7}Ni_{5.3}P_{22.5}$ BMG due to its unique properties has potential industrial applications in electrochemical devices such as micro fuel cells, energy conversion/storage and sensors [18,19]. The large ductility and high fracture toughness properties of $Pt_{57.5}Cu_{14.7}Ni_{5.3}P_{22.5}$ BMG are experimentally studied by Schroers and Johnson [20]. Chen *et al.* [21,22] reported the influence of annealing temperature on the hardness, elastic modulus and surface morphology of $Pt_{57.5}Cu_{14.7}Ni_{5.3}P_{22.5}$ BMG. Similar studies on fracture toughness variation of the BMG under consideration were also reported by Ketkaew *et al.* [23]. However, understanding and controlling the properties of bulk metallic glasses in general is limited by the lack of sound theoretical understanding for the disordered and non-equilibrium glassy materials.

In this work, we compute the phonon dispersion curves of $Pt_{57.5}Cu_{14.7}Ni_{5.3}P_{22.5}$ BMG using the simple model given by Bhatia and Singh [4] employing various dielectric screenings. This simple model proposed by Bhatia and Singh assumes a central force, effective between nearest neighbours and a volume-dependent force due to conduction electrons. Bhatia and Singh had fixed the values of force constants δ and β using the value of longitudinal and transverse sound velocities along with the calculated value of force constant κ_e as no experimental data on elastic constants were available, though they have suggested to fix these parameters from elastic constants. Subsequent theoretical study of phonon dispersion employing Bhatia and Singh approach using force constant method has also derived the force constants values in a similar way [7,10-12]. In the study presented in this paper, we fix the value of force constants δ and β used in the computation of dispersion curves by using the value of bulk modulus (B) and shear modulus (G) of the BMG under consideration for the first time along with the calculated value of force constant κ_e. The dielectric screening due to conduction electrons is quite significant in the long wavelength region of the dispersion curves and to study the effects of various dielectric screenings on the dispersion curves in longitudinal mode, we employ the dielectric screening functions [24] due to Bhatia and Singh (BS) [4], Hartree (H), Hubbard (HB), Geldart and Vosko (GV), self-consistent screening due to Shaw (SCS) [25], and Overhauser (OH) [26]. The longitudinal sound velocities (V_L) are computed for different dielectric screenings and the transverse sound velocity (V_T) is obtained which is without dielectric screening from dispersion curves in the long wavelength region. The corresponding Debye temperature (θ_D) is finally obtained for various dielectric screenings.

2. Theory

The equations for the longitudinal phonon frequencies (ω_L) and transverse phonon frequencies (ω_T) as given by Bhatia and Singh [4] are written as

$$\omega_{\mathrm{L}}^2 = \frac{2N}{\rho a^2}[\beta I_0 + \delta I_2] + \frac{\kappa_e K_{TF}^2 q^2 [G(qr_s)]^2}{\rho[q^2 + K_{TF}^2 \epsilon(q)]}, \quad (1)$$

and

$$\omega_{\mathrm{T}}^2 = \frac{2N}{\rho a^2}\left[\left(\beta + \frac{1}{2}\delta\right) I_0 - \frac{1}{2}\delta I_2\right], \quad (2)$$

here q is the momentum wave vector, a is the distance between nearest neighbours and N is the coordination number; β, δ and κ_e are force constants. β and δ are defined in terms of the first and second derivatives of inter-atomic potential $W(r)$ at $r = a$, as

$$\beta = \frac{\rho a^2}{2M}\left[\frac{1}{r}\frac{dW(r)}{dr}\right]_{r=a}, \quad (3)$$

$$\delta = \frac{\rho a^3}{2M}\left[\frac{d}{dr}\left(\frac{1}{r}\frac{dW(r)}{dr}\right)\right]_{r=a}. \quad (4)$$

In Eq. (1), the relevant force constant κ_e due to the conduction electrons based on the Thomas–Fermi model can be written as

$$\kappa_e = 4\pi n_e n_i z e^2 / K_{TF}^2, \quad (5)$$

where e is the electron charge, $n_e = n_i z$ is mean electron density and n_i is the ionic number density; $z = \sum_i C_i z_i$ is the mean valence of the glassy system, where C_i and z_i are the concentration and valence of the ith constituent; $K_{TF}^2 = (4\,k_F/\pi a_0)$ is the Thomas-Fermi screening length, where a_0 is the Bohr radius and $k_F = (3\pi^2 n_e)^{1/3}$ is the Fermi wave number.

The $[G(qr_s)]^2$ in Eq. (1) is the shape factor to take into account the cancellation effects of kinetic and potential energies inside the core of the ions and is of the form

$$[G(qr_s)]^2 = \left[\frac{3(\sin(qr_s) - (qr_s)\cos(qr_s))}{(qr_s)^3}\right]^2, \quad (6)$$

where $r_s = [3/(4\pi n_i)]^{1/3}$ is the radius of the Wigner- Seitz sphere.

To study the effects of various dielectric screenings on the longitudinal phonon dispersion curve, we employ various dielectric screenings namely Bhatia and Singh (BS), Hartree (H), Hubbard (HB), Geldart and Vosko (GV), self-consistent screening due to Shaw (SCS) and Overhauser (OH). The dielectric screening function $\epsilon(q)$ in Eq. (1) takes the following forms for various dielectric screenings.

Bhatia and Singh [4] used as

$$\epsilon(q) = \frac{1}{2}\left[1 + \frac{k_F}{q}\left(1 - \frac{q^2}{4k_F^2}\right)\mathrm{In}\left|\frac{q+2k_F}{q-2k_F}\right|\right][1 - f(q)], \quad (7)$$

where $f(q)$ is given by Hubbard [27] as

$$f(q) = \frac{1}{2}q^2/\left(q^2 + k_F^2 + \frac{1}{2}K_{TF}^2\right). \quad (8)$$

Hartree dielectric screening [24] takes the form of

$$\epsilon_H(q) = 1 + Q_0(q), \quad (9)$$

where $Q_0(q) = (K_{TF}^2/q^2)f(x)$ with $x = q/k_F$

and $f(x) = 0.5 + ((4 - x^2)/8x)\ln\left|\frac{2+x}{2-x}\right|$.

The HB, GV SCS and OH dielectric screening functions [24] are given by

$$\epsilon(q) = 1 + Q_0(q)/(1 - f(q)Q_0(q)), \quad (10)$$

where $f_{HB}(q) = 0.5q^2/(q^2 + k_F^2 + K_{TF}^2)$. (11)

$$f_{GV}(q) = 0.5q^2/(q^2 + vk_F^2) \text{ with } v = 2/[1 + .153(K_{TF}^2/4k_F^2)]. \quad (12)$$

$$f_{SCS}(q) = A[1 - \exp(-B(q/k_F)^2)] \text{ with } A = 1 \text{ and } B = 0.535. \quad (13)$$

and $f_{OH}(q) = 0.275(q/k_F)^2/[1 + 2.5(q/k_F)^2 + .09375(q/k)^4]^{1/2}$. (14)

In Eqs. (1) and (2)

$$I_n = \int_0^{\pi} \sin\theta \cos^n\theta \left[\sin^2\left(\frac{1}{2}qa\cos\theta\right)\right] d\theta, \quad (15)$$

where θ is the angle between the unit vector along the displacement of the wave and the vector joining the atom at the origin to one of its nearest neighbours,

so that with $x = qa$, I_0 and I_2 are respectively,

$$I_0(x) = 1 - \frac{\sin x}{x}, \quad (16)$$

$$I_2(x) = \frac{1}{3} - \sin x\left[\frac{1}{x} - \frac{2}{x^3}\right] - \frac{2\cos x}{x^2}, \quad (17)$$

for the limiting case $q \to 0$, $x \to 0$; $I_0(x) \approx \frac{1}{6}x^2$ and $I_2(x) \approx \frac{1}{10}x^2$. Substituting these values in Eqs. (1) and (2), we have the longitudinal and transverse sound velocities respectively, $V_L(0) = \omega_L/q$ and $V_T(0) = \omega_T/q$ in low momentum region $(q \to 0)$ as

$$\rho V_L^2(0) = N\left(\frac{1}{3}\beta + \frac{1}{5}\delta\right) + \kappa_e, \quad (18)$$

$$\rho V_T^2(0) = N\left(\frac{1}{3}\beta + \frac{1}{15}\delta\right). \quad (19)$$

In terms of the elastic moduli of the glassy material [4]

$$C_{11} = \rho V_L^2(0) = B + \frac{4}{3}G, \quad (20)$$

$$C_{44} = \rho V_T^2(0) = G. \quad (21)$$

The longitudinal sound velocities (V_L) for various dielectric screenings are obtained from the ω_L-q dispersion curves in the long wavelength region. Similarly, the transverse sound velocity (V_T) is obtained from the ω_T-q dispersion curve in the long wavelength region.The value of the Debye temperature (θ_D) is obtained using the relation [28]

$$\theta_D = \frac{h}{K_B}\left(\frac{9n_i}{4\pi}\right)^{1/3}\left(\frac{1}{V_L^3}+\frac{2}{V_T^3}\right)^{-1/3}. \quad (22)$$

3. Calculations

The experimental values of B, G and ρ are taken from Schroers and Johnson [20] for $Pt_{57.5}Cu_{14.7}Ni_{5.3}P_{22.5}$ as 198.7x10^9 Nm^{-2}, 33.3x10^9 Nm^{-2} and 15.02x10^3 kgm^{-3} respectively. The value of n_i calculated using the relation $\rho = n_i M$ is found to be 6.876 x10^{28} m^{-3}. Since the BMG under consideration is of FCC structure, n_i can be written as

$$a^3 n_i = \sqrt{2}\ . \quad (23)$$

Substituting the value of n_i in Eq. (23) gives a = 2.74x10^{-10} m. The calculated value of mean valence of the BMG using the relation $z = \sum_i C_i z_i$ is 2.08. The value of κ_e is calculated using Eq. (5) with $z = 2.08$ for $Pt_{57.5}Cu_{14.7}Ni_{5.3}P_{22.5}$ is found to be 162.198x 10^9 Nm^{-2}. The values of force constants β and δ are obtained by substituting the values of B, G and κ_e in Eqs. (18-21) taking N = 12 for FCC structure. Hence, all the values of the quantity in dispersion relations in Eqs. (1) and (2) are known. The parameters used for computing phonon dispersion curves are listed in Table 1.

Table 1. Parameters used for computing phonon dispersion curves of $Pt_{57.5}Cu_{14.7}Ni_{5.3}P_{22.5}$ BMG.

	$Pt_{57.5}Cu_{14.7}Ni_{5.3}P_{22.5}$
ρ (10^3 kgm^{-3})	15.02
n_i(10^{28} m^{-3})	6.876
κ_e (10^9 Nm^{-2})	152.198
k_F (10^{10} m^{-1})	1.618
r_s (10^{-10} m)	1.514
K_{TF}^2 (10^{20} m^{-2})	3.893
β (10^9 Nm^{-2})	2.313
δ (10^9 Nm^{-2})	36.006
z	2.08

4. Results and Discussion

The phonon dispersion relation in Eq. (1) is applied to $Pt_{57.5}Cu_{14.7}Ni_{5.3}P_{22.5}$ BMG with different dielectric screening functions viz. BS, H, HB, GV, SCS, and OH to get the longitudinal phonon frequencies. Similarly, Eq. (2) is applied to obtain the transverse phonon frequency which is without dielectric screening. The phonon dispersion curves for $Pt_{57.5}Cu_{14.7}Ni_{5.3}P_{22.5}$ BMG are shown in Fig. 1. From the Fig. 1, the longitudinal (ω_T-q) and transverse (ω_L-q) dispersion curves show linear dispersion curves in the long wavelength region.

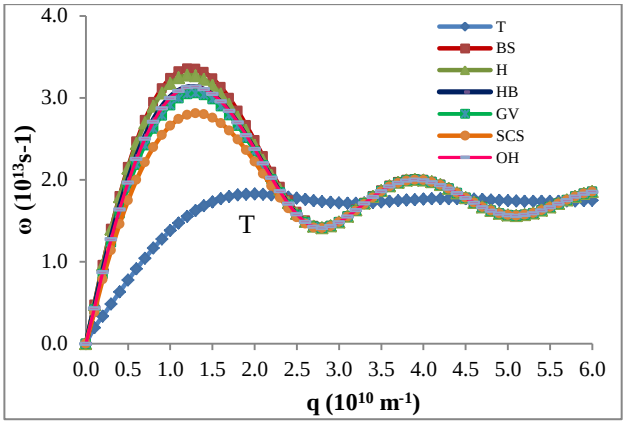

Fig. 1. The transverse (T) phonon dispersion curves on the basis of Eq. (2) and longitudinal phonon dispersion curves due to dielectric screenings viz. BS, H, HB, GV, SCS and OH on the basis of Eq. (1) for $Pt_{57.5}Cu_{14.7}Ni_{5.3}P_{22.5}$ BMG.

As seen from Fig. 1, ω_L-q dispersion curves depend on the dielectric screening employed. The position of the first peak for ω_L-q curves is found at q = 1.2x10^{10} m^{-1} for BS and H form of dielectric screenings, while for HB, GV, SCS and OH form of dielectric screenings it is found at q=1.3x10^{10} m^{-1}. The height of the peak is also dependent on the type of dielectric screenings employed. The difference in ω_L values increases as q starts increasing and it gradually widens and becomes prominent at the first maxima (peak) of the curve. The peak heights of SCS, GV, HB, OH, H and BH form of dielectric screenings are in the ascending order. For SCS the peak height is lowest while it is the highest for BS form of screening. The overall difference between SCS and BS is 19.56 %. With further increase in q, the ω_L values start decreasing and the ω_L-q curves converge at the q value corresponding to the first minima of ω_L-q curves obtained at q=2.8x10^{10} m^{-1} and it is independent of the dielectric screenings. Beyond this q value, ω_L values are independent of dielectric screenings employed. The first peak position of ω_T-q curve is obtained at q=2.0x10^{10} m^{-1} which is at higher q value than the first peak position of ω_L-q curves for all dielectric screenings. The dispersion curve of ω_T-q increases with wave number q and gets saturated around the first peak with a small variation. With further increase in q value, the damping of transverse phonons becomes prominent.

The sound velocities of the transverse and longitudinal modes are estimated for this BMG in the long wavelength region (q→0) of the dispersion curves. For estimating the sound velocities of transverse and longitudinal modes, we have taken the data range (q = 0.1 x10^{10} m^{-1} to q = 0.4 x10^{10} m^{-1}) for all the screenings. The values of sound velocities estimated from the dispersion curves for the transverse (V_T) and longitudinal (V_L) modes are listed in Table 2.

Table 2. The longitudinal (V_L) and transverse (V_T) sound velocities along with Debye temperature (θ_D) for $Pt_{57.5}Cu_{14.7}Ni_{5.3}P_{22.5}$ BMG employing different dielectric screenings.

	$Pt_{57.5}Cu_{14.7}Ni_{5.3}P_{22.5}$		
Dielectric screenings	V_L (10^5 cms^{-1})	V_T(10^5 cms^{-1})	θ_D(K)
BS	4.413	1.457	202.2
H	4.379		202.1
HB	4.112		201.9
GV	3.904		201.6
SCS	3.592		201.1
OH	4.035		201.8
Experimental	4.000 [20]	1.481 [20]	206 [2]

The value of transverse velocity computed from the slope of the dispersion curve, which is without any dielectric screening in the long wavelength region is V_T=1.457x10^5 cms^{-1}. The computed transverse sound velocity is 1.6 % less than the experimental value of 1.481x10^5 cms^{-1} reported by Schroers and Johnson [20]. Similarly, the values of longitudinal velocities (V_L) computed for various dielectric screening are listed in Table 2. The screenings due to various dielectric screening functions have an effect on the longitudinal sound velocity. However the values of longitudinal sound velocities computed from the dispersion curves are close to the experimental value of 4.000 x10^5 cms^{-1} [20] with the dielectric screening due to OH showing nearest to the experimental value. The corresponding Debye temperature, θ_D(K) is computed using Eq. (22) by substituting the value of transverse sound velocity which is without dielectric screening and the longitudinal sound velocity values for various dielectric screenings as listed in Table 2. There is not much variation in the computed values of θ_D for different dielectric screening function and it is very close to the reported value of 206 K [2].

The position of the first minimum of ω_L-q curves lie where the first peak (q_p) of the static structure factor, $S(q)$ is predicted. The position of the first minimum of ω_L-q curves lies at q= 2.8x10^{10} m^{-1} and is independent of the dielectric screenings. Since no experimental data for the static structure factor of $Pt_{57.5}Cu_{14.7}Ni_{5.3}P_{22.5}$ BMG is available, we predicted from our theoretical phonon dispersion curves to be around q = 2.8x10^{10} m^{-1}. Moreover, the computed value of q_p for the system under consideration is slightly less than $2k_F$, where k_F = 1.618x10^{10} m^{-1} is the calculated value of the BMG as shown in Table 1. The ratio of $2k_F/q_p$=1.15 for this BMG is in good agreement with the stability of metallic glasses [29]**.** The structure factor provided key structural information on the atomic network for amorphous matters and a universal relationship exists between the elastic properties and the wavelength λ (i.e. $2\pi/q_p$) [3]. Since the experimental data for phonon frequencies are rare and the limitation of the experimental techniques for describing the micro-structure of metallic glasses, it is expected that theoretical computation of phonon dispersion curves will give insight on understanding the structural information and elastic properties of metallic glasses.

4. Conclusion

We theoretically investigated the phonon dispersion curves of $Pt_{57.5}Cu_{14.7}Ni_{5.3}P_{22.5}$ BMG employing various dielectric screenings using the Bhatia and Singh approach. In computing the dispersion curves we have fixed the values of force constants δ and β using the experimental values of bulk modulus (B) and shear modulus (G) along with the calculated value of force constant κ_e of the BMG under consideration. This method of fixing force constants is applied for the first time. From the computed dispersion curve, the acoustic and thermodynamic properties along with the position of the first peak of static structure factor can be predicted. The values of sound velocities and Debye temperature computed from the phonon dispersion curves of $Pt_{57.5}Cu_{14.7}Ni_{5.3}P_{22.5}$ BMG using this method is in good agreement with the experimental data. Thus, in view of the excellent agreement with the experimental data, we plead for the reliability of the results computed by this method and we are presently working on applying this method for computing phonon dispersion curves of other BMGs.

References

1. A. Inoue, Acta Mater. **48**, 279 (2000). https://doi.org/10.1016/S1359-6454(99)00300-6
2. W. H. Wang, Prog. Mater. Sci. **57**, 487 (2012). https://doi.org/10.1016/j.pmatsci.2011.07.001
3. Y. Wu, H. Wang, Y. Cheng, X. Liu, X. Hui, T. Nieh, Y. Wang, and Z. Lu, Sci. Rep. **5**, 12137 (2015). https://doi.org/10.1038/srep12137
4. A. B. Bhatia and R. N. Singh, Phys. Rev. B **31**, 4751 (1985). https://doi.org/10.1103/PhysRevB.31.4751
5. A. L. Greer, Nature **366**, 303 (1993). https://doi.org/10.1038/366303a0
6. A. Paul, A. K. Chattopadhyay, and C. Basu, J. Appl. Phys. **84**, 2513 (1998). https://doi.org/10.1063/1.368412
7. P. C. Agarwal, K. A. Azez, and C. M. Kachhava, Acta Phys. Hung. **71**, 233 (1992). https://doi.org/10.1007/BF03054282
8. R. Babilas, D. Lukowiec, and L. Temleitner, Beilstein J. Nanotechnol. **8**, 1174 (2017). doi:10.3762/bjnano.8.119
9. A. Gulenko, L. F. Chungong, J. Gao, I.Todd, A.C. Hannon, R. A. Martin, and J. K. Christie, Phys. Chem. Chem. Phys. **19**, 8504 (2017). https://doi.org/10.1039/C6CP03261C
10. P. C. Agarwal, Physica B **381**, 239 (2006). https://doi.org/10.1016/j.physb.2006.01.522
11. P. C. Agarwal, Mater. Sci. Eng. A **404**, 301 (2005). https://doi.org/10.1016/j.msea.2005.05.073
12. P. C. Agarwal, Comput. Mater. Sci. **42**, 619 (2008). https://doi.org/10.1016/j.commatsci.2007.09.016
13. A. M. Vora and A. L. Gandhi, Armen. J. Phys. **12**, 289 (2019).
14. J. Hubbard and J. L. Beeby, J. Phys. C **2**, 556 (1969). https://doi.org/10.1088/0022-3719/2/3/318
15. S. Takeno and M. Goda, Prog. Theor. Phys. **45**, 331 (1971). https://doi.org/10.1143/PTP.45.331
16. A. Pratap, D. Bhandari, and N. S. Saxena, Mater. Sci. Eng. A **375–377**, 697 (2004) https://doi.org/10.1016/j.msea.2003.10.171
17. K. N. Lad and A. Pratap, Physica. B **334**, 135 (2003). https://doi.org/10.1016/S0921-4526(03)00039-5
18. M. Carmo, R. C. Sekol, S. Ding, G. Kumar, J. Schroers, and A. D. Taylor, ACS Nano **5**, 2979 (2011). https://doi.org/10.1021/nn200033c

19. R. C. Sekol, G. Kumar, M. Carmo, F. Gittleson, N. Hardesty-Dyck, S. Mukherjee, J. Schroers, and A. D. Taylor, Small **9**, 2081 (2013). https://doi.org/10.1002/smll.201201647
20. J. Schroers and W. L. Johnson, Phys. Rev. Lett. **93**, ID 255506 (2004). https://doi.org/10.1103/PhysRevLett.93.255506
21. Z. Chen, A. Datye, P. A. Brooks, M. Sprole, J. Ketkaew, S. Sohn, J. Schroers, and U. D. Schwarz, MRS Adv. **4**, 73 (2019). https://d19.30oi.org/10.1557/adv.20
22. Z. Chen, A. Datye, J. Ketkaew, S. Sohn, C. Zhou, O. E. Dagdeviren, J. Schroers, and U.D. Schwarz, Scripta Mater. **182**, 32 (2020). https://doi.org/10.1016/j.scriptamat.2020.02.035
23. J. Ketkaew, W. Chen, H. Wang, A. Datye, M. Fan, G. Pereira, U. D. Schwarz, Z. Liu, R. Yamada, W. Dmowski, and M. D. Shattuck, Nat. Commun. **9**, 1 (2018). https://doi.org/10.1038/s41467-018-05682-8
24. P. C. Agarwal, K. A. Aziz, and C. M. Kachhava, Acta Phys. Hung. **72**, 183 (1992). https://doi.org/10.1007/BF03054162
25. R. W. Shaw Jr., J. Phys. C **3**, 1140 (1970). https://doi.org/10.1088/0022-3719/3/5/027
26. A. W. Overhauser, Phys. Rev. B **3**, 1888 (1971). https://doi.org/10.1103/PhysRevB.3.1888
27. J. Hubbard, Proceed. Royal. Soc. A **243**, 336 (1958). https://doi.org/10.1098/rspa.1958.0003
28. J. Hafner, Phys. Rev. B **27**, 678 (1983). https://doi.org/10.1103/PhysRevB.27.678
29. W. H. Wang, C. Dong, and C. H. Shek, Mater. Sci. Eng. R: Reports **44**, 45 (2004). https://doi.org/10.1016/j.mser.2004.03.001